



## Editorial

## The Journal of Cardiovascular Computed Tomography: 2020 Year in review



## ARTICLE INFO

## Keywords

Cardiac computed tomography  
 Cardiac CT  
 Coronary artery calcium  
 Coronary CT angiography  
 COVID-19  
 Journal of cardiovascular computed tomography  
 Structural heart disease

## ABSTRACT

The purpose of this review is to highlight the most impactful, educational, and frequently downloaded articles published in the Journal of Cardiovascular Computed Tomography (JCCT) for the year 2020. The JCCT reached new records in 2020 for the number of research submissions, published manuscripts, article downloads and social media impressions. The articles in this review were selected by the Editorial Board of the JCCT and are comprised predominately of original research publications in the following categories: Coronavirus disease 2019 (COVID-19), coronary artery disease, coronary physiology, structural heart disease, and technical advances. The Editorial Board would like to thank each of the authors, peer-reviewers and the readers of JCCT for making 2020 one of the most successful years in its history, despite the challenging circumstances of the global COVID-19 pandemic.

## 1. Introduction

The global coronavirus disease 2019 (COVID-19) pandemic has significantly disrupted the worldwide delivery of healthcare, cardiovascular disease research, and medical education. Despite these challenges, the field of cardiovascular computed tomography (CCT) has continued to grow at an accelerated pace, with a wide array of innovations, novel insights and knowledge gained. The year 2020 was a productive and exciting one for the *Journal of Cardiovascular Computed Tomography* (JCCT), with the journal reaching records in the number of journal submissions, online article views and downloads, social media engagements (Table 1), published manuscripts and case reports.<sup>1,2</sup> The purpose of this review is to summarize some of the most impactful and educational work published in the print issues of the JCCT during 2020, as selected by the Editorial Board.

## 2. COVID-19

To meet the unique challenges faced by those providing cardiovascular imaging care during the pandemic, the practice of CCT evolved in 2020. Based on its high diagnostic accuracy, rapid non-invasive acquisition, low cost, and safety for patients and staff, international guidelines and statements from professional Societies now recommend an increasingly prominent role for CCT.<sup>3–5</sup>

Shortly after the onset of the COVID-19 pandemic, the Society of Cardiovascular Computed Tomography (SCCT) convened an expert panel to provide guidance on the performance of CCT during the pandemic.<sup>6</sup> This document, which was endorsed by the American College of Cardiology, detailed important patient and CCT staff member safety practices, indications for CCT that may be safely deferred, and situations where CCT may be the preferred modality to reduce potential COVID-19 virus exposure to staff and patients, as well as to more rapidly diagnose and

treat patients with known or suspected cardiovascular diseases. Specifically, this document recommended increased utilization of CCT in lieu of transesophageal echocardiography (TEE) for the evaluation of intracardiac thrombus prior to cardioversion in patients with atrial arrhythmias. The authors also recommended first-line performance of coronary CT angiography (CTA) as an alternative to functional tests for ischemia and invasive coronary angiography (catheterization) in appropriately selected symptomatic patients in order to most rapidly and accurately assess for acute coronary syndrome and/or high risk stable coronary artery disease. The goal of these recommendations was also to avoid unnecessary admissions, catheterizations and staff exposure to potentially infected patients as can be seen during stress testing or invasive procedures.

In a similar fashion, a group of experts led by Drs. Kanwal Farooqi and Kelly Han published a document on the use of CCT for congenital heart diseases during the COVID-19 pandemic. This timely document classified indications for CCT in patients with congenital heart disease as urgent (timing of CCT <7 days), semi-urgent (timing of CCT <4 weeks) and non-urgent (timing of scan <3 months), as well as defining several conditions where routine CCT surveillance can be delayed beyond 6 months.<sup>7</sup>

Of note, this field is currently under ongoing investigations, with new data appearing monthly. Systematic data collections from large cohorts are needed in order to define the role of CCT in COVID-19 beyond its established use for the evaluation of pulmonary involvement and to rule out acute coronary syndrome. The documents published are aimed to provide an “emergent” guide for an emergency situation, but are not yet backed-up by larger systematic data collections. The exact clinical indications – when to use CT or cardiac magnetic resonance imaging (CMR) – have yet to be defined. SARS-CoV-2 causes “myocardial injury” by distinct pathways including myocardial inflammation, systemic hyper-inflammatory response (SIRS) and/or microthrombotic processes (small vessel disease), hence both modalities CT and CMR have a promising

<https://doi.org/10.1016/j.jcct.2021.02.004>

Available online 22 February 2021

1934-5925/© 2021 Society of Cardiovascular Computed Tomography. Published by Elsevier Inc. All rights reserved.

**Table 1**

Top 10 journal of cardiovascular computed tomography top social media (by engagement) for 2020.

Article (Type) Author	Engagement
Screening for atherosclerosis among low risk individuals with family history of CHD (Editorial) Daly R, Blankstein R	166
Dynamic CT assessment of mitral annulus in patients with and w/o mitral prolapse (Research) Rizvi A, Williamson E et al.	125
SCCT guidance for CT Amidst COVID-19: Endorsed by ACC (Guideline) Choi AD, Blankstein R et al.	112
LAA Morphology is Associated with embolic stroke subtypes using a simple classification system (Research); Yaghi S, Atalay MK et al.	104
ISCHEMIA Trial: Implications for coronary CT angiography (Editorial) Blankstein R, Shaw LJ	104
Feasibility of measuring pericoronary fat from precontrast scans: Effect of iodinated contrast (Research) Almeida S, Budoff M et al.	94
The impact of the COVID-19 pandemic on cardiac CT (President's Page) Blankstein R	78
Baseline global longitudinal strain by CT is associated with post TAVR outcomes (Research) Fukui M, Cavalcante J et al.	65
Coronary artery calcium: A Modern rubric for an established approach (Editorial) Al'Aref, Choi AD, Villines T	59
The not so secret power of cardiac CT: Prevention and value (Editorial) Blankstein R, Shaw LJ, Nasir K	48

Social media engagement allows for assessment of the initial impact and attention of articles published in the *Journal of Cardiovascular Computed Tomography* (JCCT). Shown are the top 10 articles by social media engagement (by PlumX) as defined as the number of Twitter retweets, Facebook likes and comments. Analyzed Jan 9, 2021 for articles published in 2020 print issues of the JCCT.

potential in clinical practice.

### 3. Coronary artery disease

#### 3.1. Coronary artery calcium scanning

The Coronary Artery Calcium Data and Reporting System (CAC-DRS) is an SCCT-developed structured reporting system for coronary artery calcium (CAC) scans that includes the Agatston score (A) and the number of vessels (N) with calcified atherosclerosis, as well as CAC scoring methodology for non-gated, non-contrast chest CT scans.<sup>5</sup> Validation of its prognostic usefulness beyond the Agatston score or number of involved vessels had not previously been performed. Dzayc and colleagues from the CAC Consortium assessed the prognostic accuracy of CAC-DRS in 54,678 patients (mean age 54 years; 34% female) for the outcomes of all-cause, coronary and cardiovascular disease mortality over a median of 12 years of follow-up.<sup>9</sup> There was a graded increased risk for all definitions of mortality with increasing CAC-DRS groups, ranging from an all-cause mortality rate of 1.2 per 1000 person-years for A0 to 15.4 per 1000 person-years for A3/N4. CAC-DRS was superior to traditional Agatston CAC categories (area under the curve [AUC] 0.762 vs. 0.754,  $p < 0.001$ ) and CAC distribution (AUC 0.762 vs. 0.748,  $p < 0.001$ ).

In an analysis from the SCOT-HEART (Scottish COmputed Tomography of the HEART) study, Dr. Williams and colleagues assessed the prognostic value of both CAC-DRS and CAD-RADS (Coronary Artery Disease Reporting and Data System)<sup>10</sup> in 1769 subjects for prediction of myocardial infarction (MI) at 5 years.<sup>11</sup> This sub-study aimed to assess if these reporting systems, designed to both standardize CAC and coronary CTA reporting and link study findings to appropriate management recommendations, also provided incremental prognostic value across the range of severity scores. The authors found that patients with low CAC-DRS or CAD-RADS scores have a low risk of subsequent cardiac

events. In contrast, those in the highest CAC-DRS and CAD-RADS categories were greater than 9 times more likely to suffer fatal or non-fatal myocardial infarction than those with the lowest score.

The use of age and sex based CAC percentiles is commonly utilized to compare a patients' Agatston CAC score to that of patients of similar age and sex. However, the available reference CAC percentiles are based on single studies which limits generalizability. De Ronde and colleagues conducted a pooled analysis that included 12 studies involving 134,336 Western (89% United States) and 33,488 Asian (92% Korean) patients from which separate weighted CAC percentiles were calculated.<sup>12</sup> The authors published this updated CAC percentile nomogram at <https://www.calciumscorecalculator.com> with the goal of providing the field with a more applicable, generalizable CAC percentile calculator.

The use of non-contrast CCT for assessment of CAC in symptomatic patients remains controversial based on clinical concerns that CAC testing may miss angiographically and prognostically significant coronary atherosclerosis. Senoner and colleagues performed a single-center, retrospective analysis of 1451 patients referred for testing based on clinical suspicion of CAD and found to have a CAC score  $< 1$  (CAC = 0 in 1289, CAC  $< 1$  in 162).<sup>13</sup> In this cohort, 66% were symptomatic and 33% were without symptoms but referred based on suspected CAD following abnormal results of cardiac testing. The presence of stenosis, plaque, and high-risk plaque ( $\geq 2$  of low-attenuation plaque [ $< 90$  Hounsfield units, HU], napkin ring sign, spotty calcification or positive remodeling) was assessed. The authors reported that in patients without CAC (CAC = 0), 25.9% of patients had evidence of coronary atherosclerosis on coronary CTA, 6.8% had high-risk plaque, and 5% had a coronary artery stenosis  $\geq 50\%$  (Fig. 1). These findings were similar to that seen in the previously mentioned SCOT-HEART analysis (above) where 17% of subjects with CAC-DRS of zero were found to have CAD on coronary CTA (CAD-RADS 1 or above).<sup>11</sup> Taken together, these results challenge the use of CAC testing in symptomatic patients, particularly when low-radiation dose, high-quality coronary CTA is available.

#### 3.2. Coronary CTA

##### 3.2.1. The ROMICAT-II (rule out myocardial infarction/ischemia using computer

Assisted Tomography) study investigators assessed the short-term and lifetime cost-effectiveness of coronary CTA versus standard of care using individual data from 1000 trial participants at low-to-intermediate risk for acute coronary syndrome (ACS) who presented to the emergency department (ED) with acute chest pain.<sup>14</sup> The authors assessed cost-effectiveness using a Markov microsimulation model based on observed trial outcomes and estimates of long-term treatment effects and medication and cardiac procedural costs. Costs and rates of coronary revascularization within 1 month of ED presentation were higher with coronary CTA, \$4490 vs. \$2513-\$4,144, and 5.2% vs. 2.6%–3.7%, respectively. However, over a lifetime, coronary CTA dominated the standard of care approach and was cost effective (\$49,428/QALY). This was due to an early and accurate detection of true CAD status by coronary CTA that resulted in a reduction in cardiovascular mortality 3 years after the initial ED presentation based mainly through more appropriate preventive medical therapy.

The most common method utilized clinically for assessing and reporting CAD disease severity on coronary CTA is based on the worst lumen stenosis.<sup>10</sup> Van den Hoogen and the CONFIRM (COronary CT Angiography Evaluation For Clinical Outcomes: an International Multicenter) registry investigators performed a nested case-control study that compared the prognostic accuracy of worst stenosis, CAD-RADS, and multiple risk scores derived from coronary CTA that quantify the overall burden of CAD plus stenosis severity, for prediction of 5-year events.<sup>15</sup> In 1464 patients propensity matched according to the presence or absence of diabetes, the authors demonstrated that compared to stenosis severity (any stenosis  $\geq 50\%$  or  $\geq 70\%$ ), semi-quantitative risk scores had the highest discriminatory ability in diabetic and non-diabetic patients and

the highest AUC compared to stenosis or CAD-RADS in diabetic patients. This analysis suggests that future iterations of CAD-RADS should consider incorporating the extent of coronary atherosclerosis and location of stenosis in addition to only worst stenosis for most accurately predicting individual patient risk and guiding therapies.

Coronary plaque volume quantification on CTA is a hot topic in the field of cardiovascular imaging and prevention, with numerous articles recently published in the JCCT on this dynamic subject.<sup>16–20</sup> In an analysis from the PARADIGM (Progression of Atherosclerotic Plaque Determined by Computed Tomographic Angiography IMaging) study, investigators assessed three techniques for quantifying plaque burden: (1) total plaque volume (PV) in mm<sup>3</sup>, (2) percent atheroma volume (PAV) in % (PV/vessel volume \* 100%), and (3) normalized total atheroma volume in mm<sup>3</sup> (PV/vessel length \* mean population vessel length). The authors report that in a large sample (1479 patients) who underwent baseline CTA, PAV was less affected by patient body surface area than the other two measures. As the method that may best account for differences in coronary artery sizes, the authors conclude that PAV is the preferred method when reporting quantitative coronary artery plaque volume. Further studies comparing plaque quantification methods for risk prediction, as well as defining population normal values of atherosclerotic burden and plaque types are needed.

The progression of coronary atherosclerosis using quantitative plaque assessment CTA is increasingly utilized to better understand cohorts at increased cardiovascular risk, as well as the biologic effects of medical therapies. Foldyna and colleagues assessed 92 individual plaques in 37 adults with human immunodeficiency virus (HIV) and subclinical CAD who were randomized to receive placebo or atorvastatin 40 mg daily.<sup>21</sup> The authors observed that statin use was associated with significantly increased rates of plaque regression (49% vs 24%, p = 0.016) and a substantial decrease in the number of proximal coronary artery plaques with progression. The authors conclude, from this substudy of a

randomized controlled trial (NCT00965185), that in an HIV population with subclinical coronary atherosclerosis who are known to be at higher than average cardiovascular risk, individual coronary plaque changes vary within a given individual and that statins act to stabilize progressing plaques by reducing fatty and fibrotic plaque components.

Coronary CTA has known high diagnostic accuracy for the assessment of coronary artery bypass graft (CABG) conduits. However, the accuracy of CTA in native coronary segments in patients with prior CABG as compared to invasive coronary angiography is known to be lower related to the high burden of calcified plaque. Prior studies assessing the diagnostic accuracy of CTA in this population are limited by older scanner technology that did not include iterative reconstruction, large volume coverage, advanced detectors, and faster temporal resolution, significant advances that may improve the diagnostic accuracy of CTA in this population. Mushtaq and colleagues prospectively evaluated the accuracy of 256-detector row CTA in 300 consecutive patients with prior CABG at a single expert center in Milan, Italy.<sup>22</sup> Studies were assessed for image quality and interpretability, with diagnostic accuracy compared to ICA in 100 subjects. Interestingly, mean heart rate was ~70 bpm, with 70 patients imaged in atrial fibrillation. The authors report that 100% of bypass grafts were assessable on CTA and that CTA demonstrated 100% of graft stenoses found on ICA. In native coronary arteries, interpretability of native coronary segments was 95.6%. The sensitivity, specificity, positive predictive value, negative predictive value and accuracy of coronary arteries were 98.3%, 97.4%, 93.1%, 99.3% and 96.5%, respectively, with the overall per-patient diagnostic accuracy of 95.2%. The mean estimated effective radiation dose was 3.14 ± 1.7 mSv (using a chest k factor of 0.014). This study suggests that diagnostic accuracy of native coronary artery segments may be better than prior reports when performed using more advanced scanner platforms.

In the November-December issue, Ahn and colleagues reported the results of a single-center, prospective, observational study where they

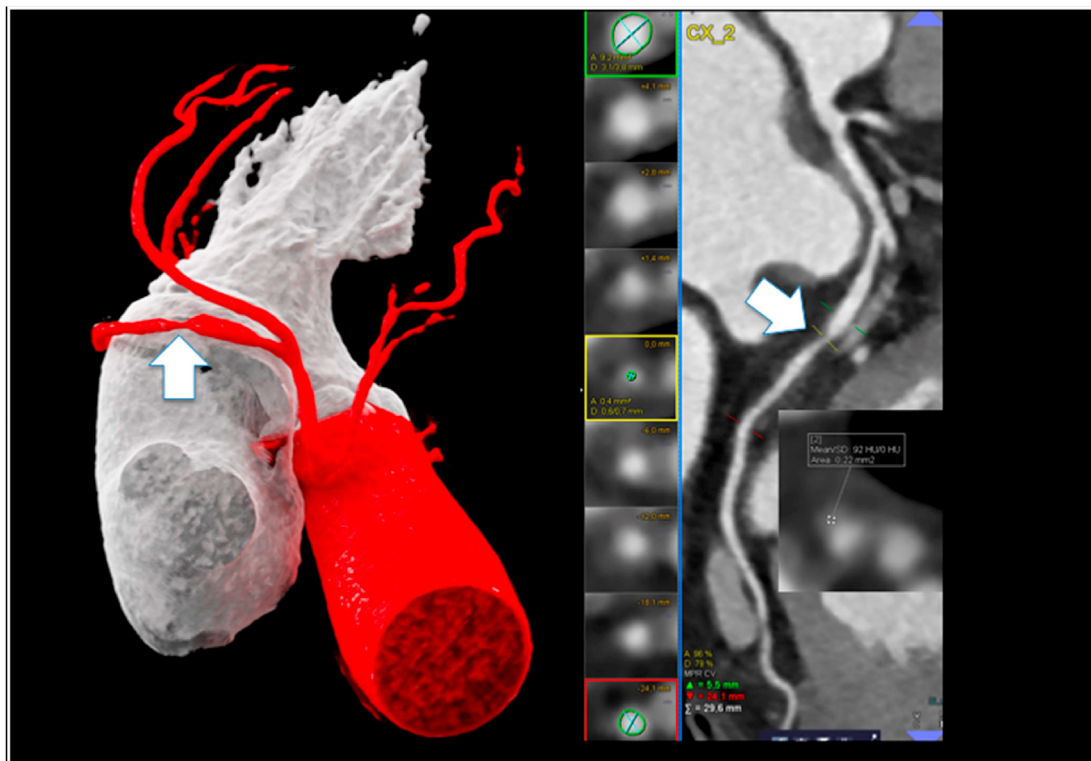


**Fig. 1.** Shows a 53-year-old male, active smoker (40 pack/years), atypical chest pain. Coronary calcium score (CCS) was zero and non-calcified lesion in the mid CX (arrows) with positive remodeling and low-attenuation fibroatheroma (92 HU) and high-grade stenosis was found. (VRT left and cMRP right). Patient died due to acute transmural myocardial infarction 23 days after CTA prior to ICA. Left dominant supply. Reproduced from reference # 21.

performed dobutamine stress echocardiogram (DSE) and coronary CTA in 206 patients scheduled to undergo non-cardiac surgery and who had at least 1 major risk factor for perioperative adverse cardiovascular events.<sup>23</sup> Ischemic heart disease was present in 35% of subjects and 87% had a revised cardiac risk index score (RCRI) of 1 (51.9%) or 2 (35.4%). DSE was abnormal in 24% of subjects and 22% had a stenosis  $\geq 50\%$  on coronary CTA, with no patients undergoing subsequent pre-operative coronary revascularization. Within 30 days following surgery, 24 subjects suffered a major perioperative cardiovascular event using a broad event definition (1 cardiac death, 10 non-fatal MI, 8 myocardial injury, 1 stroke and 1 pulmonary embolism). After adjustment for baseline RCRI, abnormal result on DSE (OR 6.08; 95% CI, 2.41–15.31), stenosis  $\geq 50\%$  on CTA (OR 18.79; 5.24–67.42), and high CACS (score  $\geq 203$ , OR 4.19; 1.39–12.60) were significant predictors of the combined occurrence of perioperative CV events. This study is the first to compare DSE to coronary CTA for the prediction of perioperative events and highlights the strong prognostic value of CAD severity on CTA for the prediction of perioperative events.

In a single-center, retrospective observational study, Drs. Hull, Thomas and colleagues reported the association of structured CTA reporting using CAD-RADS to changes in statin and aspirin following the institutional adoption of CAD-RADS reporting.<sup>24</sup> The authors observed that statin initiation or dose escalation was more common in the

CAD-RADS period (adjusted OR 1.46; 95% CI 1.12–1.90), mainly driven by new statin prescriptions in those with CAD on CTA. The authors also observed slight reductions in post-CTA cholesterol values (compared to pre-CTA values) following the institution of CAD-RADS reporting. The study, while potentially confounded by changes in lipid management guidelines unrelated to CAD-RADS and its single-center nature, highlights the possible positive effect that structured CTA reporting with management recommendations may have in patients with coronary atherosclerosis on CTA.

Pericoronary fat attenuation (PCAT) as measured on coronary CTA has recently been described as a novel measure of pericoronary inflammation and cardiovascular risk. Initial studies have utilized contrast-enhanced CTA for assessing the pericoronary contrast value and gradient. In the *November-December* issue, Almeida and colleagues assessed pericoronary attenuation ( $-190$  to  $-30$  Hounsfield units [HU]) and fat volume in 119 paired thin-slice pre-contrast and contrast cardiac CT studies (all 120 kVp) at 10–50 mm from the ostium of the right coronary artery (Fig. 2).<sup>25</sup> This novel study demonstrated that there was high inter- and intra-reader agreement for measuring mean attenuation and pericoronary fat volume for both pre-contrast and contrast studies. There was a small difference in mean PCAT on pre- and post-contrast images,  $-87.02 \pm 7.15$  HU and  $-82.74 \pm 6.54$  HU, respectively ( $p < 0.0001$ ). The authors conclude that pericoronary fat enhances with

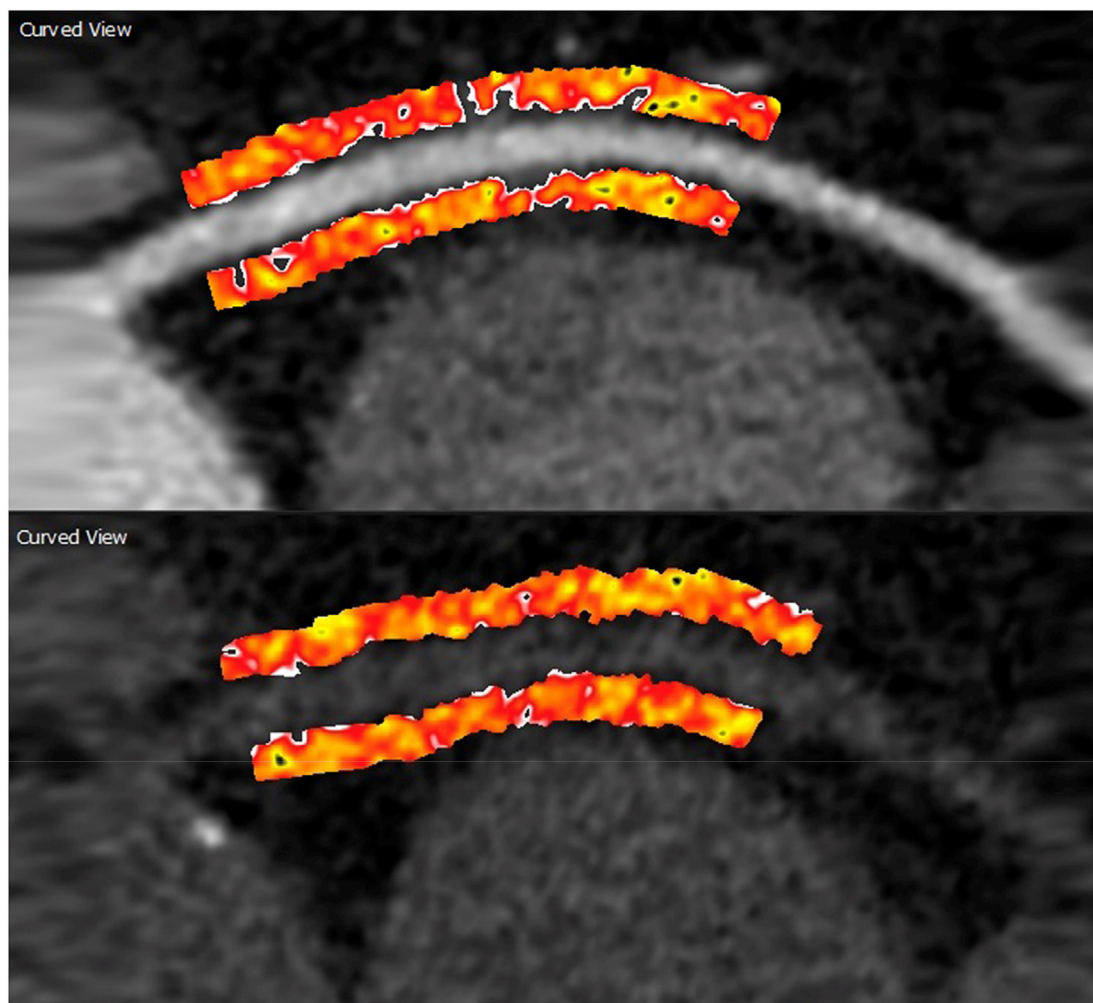


**Fig. 2.** Pericoronary fat attenuation and volume quantification on pre- and post contrast CT. Fat was defined as  $-30$  to  $-190$  HU and from 10 to 50 mm distal to the RCA origin at a radial distance equal to the vessel diameter. Reproduced from reference # 25.

iodinated contrast, but can be reliably measured on non-contrast CT studies.

#### 4. Coronary physiology

In the *January-February* issue, the SCCT published its first ever expert consensus statement on the performance on myocardial CT perfusion (CTP) imaging.<sup>26</sup> Led by Drs. Patel and Blankstein, this document summarized the current literature that guides the appropriate use of myocardial CTP, and provided readers with detailed recommendations for the optimal acquisition, interpretation, and reporting of CTP studies. This document is complemented by three state-of-the-art reviews on myocardial CTP that appeared in the JCCT during 2020.<sup>27–29</sup> These invited reviews directly compared important differences between static and dynamic CTP acquisition techniques and different scanner platforms, detailed the calculation of myocardial blood flow (MBF), as well as covered important additional technical details for those who want to learn more about this burgeoning CT technique.

In an effort to better define methodologies for assessing MBF, Yi and colleagues compared absolute versus relative measures of MBF from dynamic CTP for the detection of ischemia as defined using invasive fractional flow reserve (FFR) in 60 patients (151 vessels).<sup>30</sup> The authors utilized prototype software for semiautomated, quantitative measurements of MBF at the endocardial level and determined optimal sensitivity and specificity MBF thresholds to detect invasive FFR  $\leq 0.80$ . The sensitivity, specificity, PPV, NPV and diagnostic accuracy for the absolute endocardial MBF value and relative MBF ratio were 82.8%, 98.9%, 98.0%, 90.2%, and 92.7% and 74.1%, 93.6%, 87.8%, 85.3%, and 86.1%, respectively. The authors conclude that using this semiautomated software and absolute MBF from the endocardium was superior to relative

MBF ratio for the detection of ischemia. In a separate, complementary study from this group, the authors concluded that calculation of MBF was most accurate when performed using the endocardial layer of the myocardium, as opposed to the transmural layers for the detection of functionally significant coronary lesions.<sup>31</sup>

Topics related to computational modeling of wall or endothelial shear stress, the frictional force acting on the coronary lumen wall, on plaque growth and patient cardiovascular risk are an increasing area of investigation. In the September–October issue, Drs. Samady, Stone and colleagues provided a state-of-the-art review on the topic of wall shear stress (WSS), review intravascular studies of WSS, and discuss the use of coronary CTA for the calculation of wall shear stress.<sup>32</sup> The authors highlight, for example, the increased risk for plaque growth in areas of low WSS and the potential prognostic implications of CCT-derived WSS (Fig. 3). This issue also included an original investigation by Mizukami et al. compared the measurement of epicardial resistance by “pullback curves” from computational fluid modeling by coronary CTA with ICA. A good correlation of both modalities was found.<sup>33</sup> This curve may help to better identify the site of maximum stenosis that may benefit from revascularization, and to distinguish focal lesions from diffuse disease.

#### 5. Structural heart disease

The use of CTA to optimize the performance of transcatheter valve interventions is one of the most dynamic and exciting areas in the field of cardiovascular imaging. In the *January-February* issue, Jochheim and colleagues assessed the relationship of left ventricular outflow tract (LVOT) calcification and device-failure, defined as procedural death, valve dislocation, annulus rupture, or significant para-valvular leak (PVL), in 690 consecutive patients enrolled in a TAVR registry

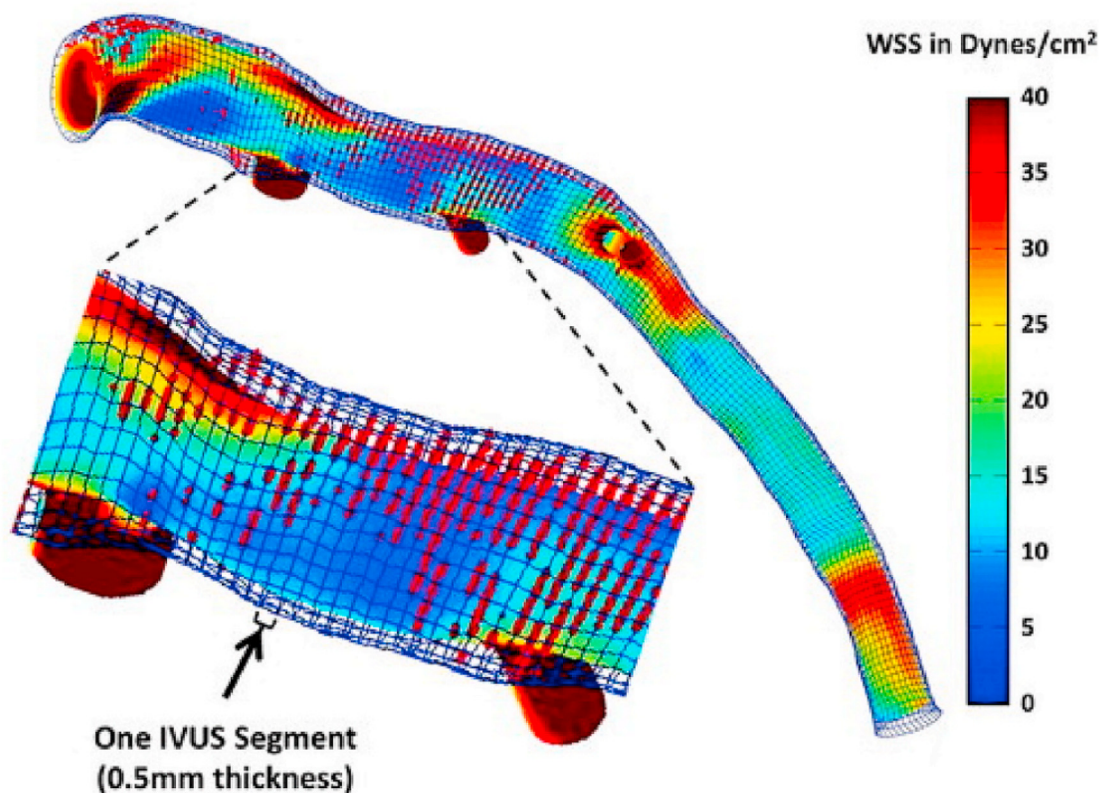


**Fig. 3.** Example of a wall shear stress (WSS) profile of the left anterior descending coronary artery from a patient demonstrating lumen and external elastic membrane boundaries, superimposed virtual histology intravascular ultrasound (IVUS)–derived necrotic core data (red dots), and areas of variable WSS. The magnified segment of the vessel demonstrates the high-resolution spatial location of the IVUS images (thickness = 0.5 mm) superimposed on the WSS profile. Time-averaged WSS values were circumferentially averaged for each IVUS segment to provide quantitative hemodynamic data to correlate with plaque progression data. Reproduced from reference #32. (For interpretation of the references to colour in this figure legend, the reader is referred to the Web version of this article.)

(NCT02289339) at a single center in Munich, Germany.<sup>34</sup> All patients (mean age 80.8 years) underwent transfemoral implantation and severe LVOT calcification was defined as a calcium volume  $\geq 609 \text{ mm}^3$  on pre-TAVR CT. Patients with severe LVOT calcification ( $n = 90$ ) experienced higher rates of post-dilation (15.6% vs. 8.5%,  $p = 0.032$ ), significant PVL (7.8% vs. 2.5%,  $p = 0.007$ ), device failure (10.0% vs. 3.8%,  $p = 0.009$ ), and 30-day mortality (10.0% vs. 2.8%,  $p < 0.001$ ). In multivariate analysis, severe LVOT calcification was an independent predictor of device failure, hazard ratio 2.87; 95% CI 1.20 to 6.34.

Pollari and colleagues performed a similar retrospective, single-center analysis of both aortic valve and LVOT calcium volume as calculated on pre-TAVR contrast-enhanced CTA and the association with in-hospital complications and long-term mortality.<sup>35</sup> Using logistic regression, the authors identified calcium load beneath the right coronary cusp in left ventricular outflow tract (LVOT) as significantly associated with stroke (OR 1.2; 1.03–1.3;  $p = 0.0019$ ) and in-hospital mortality (OR 1.1; 95% CI 1.004–1.2;  $p = 0.04$ ), whereas total calcium volume of the LVOT was associated with both in-hospital and 30 day-mortality, (OR 1.2; 1.0–1.4;  $p = 0.03$  and OR 1.2; 1.0–1.4;  $p = 0.029$ , respectively). On multivariable analysis, total calcium of LVOT (HR 1.18; 1.02–1.38;  $p = 0.026$ ), male sex (HR 1.88; 1.06–3.32;  $p = 0.031$ ), baseline creatinine clearance (HR 0.96; 0.93–0.98;  $p < 0.001$ ), and baseline severe aortic regurgitation (HR 7.48; 2.76–20.26;  $p < 0.001$ ) were independently associated with reduced survival.

Drs. Weir-McCall, Leipsic and colleagues addressed the increasingly important topic of TAVR prosthesis sizing in patients with bicuspid aortic valves.<sup>36</sup> They studied the reproducibility of supraannular versus annular measurements in 44 patients who underwent pre-TAVR CCT prior to balloon-expandable TAVR for severe aortic stenosis. The annular area (AA) was measured at the basal ring in accordance with SCCT guidelines and supraannular area (SA) was measured by generating a circle defined by the intercommisural distance (Fig. 4). All measurements performed by 2 independent observers. The authors report that the SA was significantly larger than AA ( $562 \pm 146 \text{ mm}^2$  vs.  $518 \pm 112 \text{ mm}^2$ ,  $p = 0.013$ ), with both measurements showing high inter-observer agreement. However, AA measurements showed significantly narrower limits of agreement between readers (mean difference [limits of agreement]:

AA =  $-3 \text{ mm}^2$  [22; 19], SA =  $-16 \text{ mm}^2$  [-92,76]). The authors noted no significant difference in post-TAVR gradients, significant PVL, or valve success between patients where the SA measurement would and would not have suggested a larger device and conclude that there is currently no

role for SA sizing in patients with bicuspid valves undergoing TAVR.

Most patients who undergo CCT prior to TAVR have functional datasets available for analysis. Previous work has shown that CT-derived global longitudinal strain (CT-GLS) has reasonably good correlation to GLS from echocardiography.<sup>37</sup> Gegenava and colleagues compared left ventricular (LV) GLS on echocardiography to CT-GLS in 214 patients who underwent both studies prior to TAVR (see Fig. 5).<sup>38</sup> CT-GLS was measured using a novel tissue-tracking software and dynamic CCT datasets. Mean GLS on echocardiography was  $-13.91 \pm 4.32\%$ , whereas mean feature tracking CT-GLS was  $-12.46 \pm 3.97\%$ . On Bland-Altman analysis, CT-GLS underestimated LV GLS compared to echocardiography with a mean difference of 1.44% (95% limits of agreement  $-3.85\% - 6.73\%$ ).

In an analysis assessing the prognostic value of CT-GLS, Drs. Fukui, Cavalcante, and colleagues measured global CT-GLS using a prototype software in 223 patients (mean age 83.5 years) undergoing TAVR.<sup>39</sup> Patients were followed for a median of 32 months following TAVR for all-cause mortality and a composite outcome of all-cause death and hospitalization for heart failure. The authors observed that when compared to patients with normal LVEF ( $\geq 50\%$ ) and preserved CT-GLS ( $\leq -20.5\%$ ), patients with normal LVEF but reduced CT-GLS ( $> -20.5\%$ ) had higher all-cause mortality (Chi-square 6.89,  $p = 0.032$ ) and the risk of composite outcome (Chi-square 7.80,  $p = 0.020$ ) which was no different than those with impaired LVEF. Reduced CT-GLS was independently associated with all-cause mortality (HR 1.71; 1.01–2.90;  $p = 0.049$ ) and the risk of composite outcome (HR 1.51; 1.01–2.25;  $p = 0.044$ ) on multivariable Cox regression analysis. This study highlights the potential additive prognostic value of CT-GLS in TAVR patients, particularly if echocardiographic measures of GLS are not available; however, nearly 30% of studies considered for study inclusion were not of sufficient image quality for CT-GLS analysis.

Spectral CCT may allow for significantly reduced doses of iodinated contrast across numerous cardiovascular indications. Cavallo and colleagues performed a prospective, single-center study of 116 consecutive patients undergoing CCT prior to TAVR.<sup>40</sup> All patients underwent a standard polychromatic (120 kVp) retrospectively-gated CTA using a contrast dose of 25 mL for cardiac imaging and images were compared to virtual monoenergetic images at 40 keV. The authors observed that image quality in the proximal aorta as assessed by signal to noise (SNR) and contrast to noise ratio (CNR) was significantly better on the 40 keV compared to polychromatic images (SNR  $14.65 \pm 7.37$  vs  $44.16 \pm 22.39$ ,

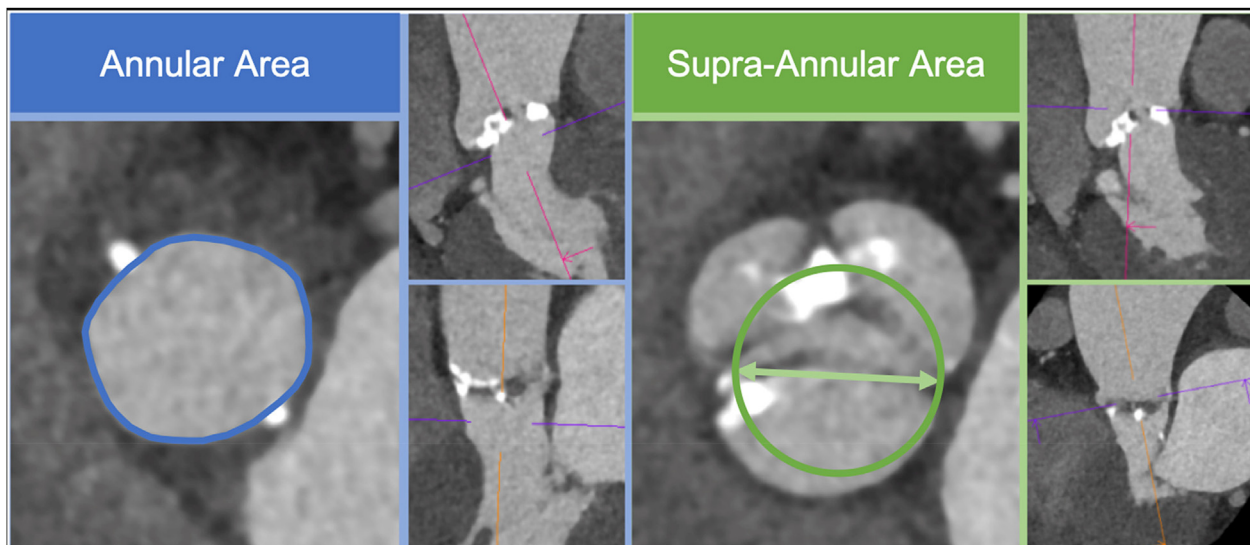
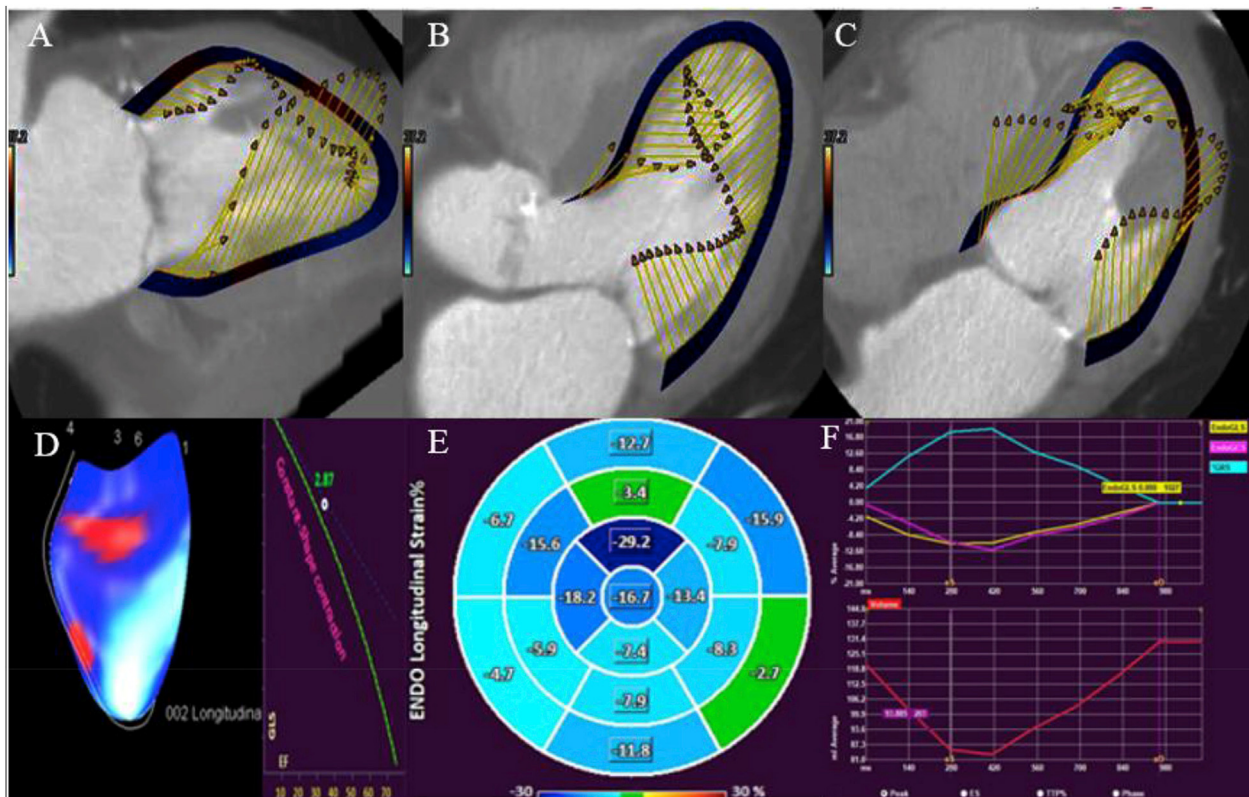


Fig. 4. Annular area and perimeter as measured at the insertion point of the 3 cusps (blue contour), and supra-annular measurement obtained using the intercommisural distance (green arrow) from which a circle is defined to allow perimeter and area calculation (green contour). Reproduced from reference #36. (For interpretation of the references to colour in this figure legend, the reader is referred to the Web version of this article.)



**Fig. 5.** Assessment of left ventricular global longitudinal strain with feature tracking multi-detector row computed tomography. Left ventricular 2-chamber (panel A), 3-chamber (panel B) and 4-chamber (panel C) views formatted via multiplanar reconstruction and processed with the help of QStrain available on Medis Suite CT. After analysing using QStrain, dynamic MDCT 3D images (panel D), Bull's eye (panel E) and strain plots (panel F) are derived. Abbreviations: EF-Ejection fraction, GLS-Global longitudinal strain, MDCT-Multidetector row computed tomography. Reproduced from reference # 38.

$p < 0.001$ ;  $CNR 15.84 \pm 9.93$  vs  $59.8 \pm 40.83$ ,  $p < 0.001$ ), with no significant differences in annular measurements. This study highlights the potential of spectral CT to allow for reduced contrast dose in patients at increased risk for contrast-induced nephropathy.

The right ventricle is visualized in most coronary CTA studies but gender-specific references to define normal volume of the RV have not been well-established. Additionally, many patients who undergo coronary CTA do so using prospective ECG triggered acquisitions at mid-diastole and reference ranges for RV size during this portion of the cardiac cycle may be useful clinically when the RV qualitatively appears enlarged. Dr. Massalha and colleagues measured RV mid-diastolic volume (RVMDV) in 1542 consecutive patients without established cardiovascular disease or prior smoking who underwent prospectively-triggered coronary CTA.<sup>41</sup> The authors report mean RVMDV for men and women was  $168.6 \pm 37.6$  mL and  $117.6 \pm 26.4$  mL, respectively. Mean BSA-indexed RVMDV was  $80.0 \pm 15.3$  mL/m<sup>2</sup> and  $64.1 \pm 12.2$  mL/m<sup>2</sup> for men and women, respectively. This study represents the largest study of normal reference mid-diastolic RV volumes currently available and may serve as a reference if RV volumes are measured on mid-diastolic scans.

Finally, Morris *et al* investigated the performance of CTA to predict PVL after transcatheter mitral valve replacement (TMVR) in 58 patients.<sup>42</sup> TMVR is a novel approach for treatment of mitral valve disease, with a variety of major technical challenges. Computational modeling of CTA data was helpful to predict PVL after TMVR.

### 6. Technical advances

There was a large number of published articles in the JCCT during 2020 that documented technical advances that are likely to improve the

quality and safety of CCT going forward.

Coronary artery calcium scoring according to the Agatston method is performed using tube potential of 120 kVp. Efforts to reduce radiation exposure from calcium scoring through the use of lower kVp settings have not been well-validated and have typically required adjustment to calcium scoring methods such that a higher HU threshold for CAC is utilized. Vingiani and colleagues investigated the accuracy of CAC scoring using 100 kVp and a tin filter (Sn100kV) with kVp-independent iterative reconstruction as compared to traditional 120 kVp Agatston scoring in 114 patients who underwent two CAC scans.<sup>43</sup> Importantly, the investigators state that the kVp-independent algorithm allows minimization of the effects of the kVp level on Agatston scores, such that the traditional 130 HU threshold can be utilized. The investigators found that median Agatston scores derived from the Sn100kV protocol with the kV-independent algorithm and the standard 120 kVp were 21.4 (IQR 0–173.8) and 24.7 (IQR 0–171.1) Agatston units respectively ( $p = 0.18$ ). Agatston scores derived from the two different protocols had an excellent correlation ( $r = 0.99$ ). The dose-length-product was  $11.5 \pm 4.1$  mGy  $\times$  cm using Sn100kV and  $50.4 \pm 24.9$  mGy  $\times$  cm using the standard 120 kVp protocol ( $p < 0.01$ ), resulting in a significantly lower (77%) effective dose at Sn100kV ( $0.16 \pm 0.06$  mSv vs.  $0.71 \pm 0.35$  mSv,  $p < 0.01$ ). Additionally, 99% of the patients were classified into the same risk category (0, 1–10, 11–100, 101–400, or >400) using the Sn100kV protocol. This study suggests that CAC doses may be significantly reduced using this novel technique but requires validation in a significantly larger population.

Benz and colleagues compared a deep-learning image reconstruction (DLIR) algorithm to adaptive statistical iterative reconstruction-Veo (ASiR-V) on image noise, image quality, and lumen narrowing in 43 patients.<sup>44</sup> High definition and standard kernels were used for ASiR-V

and varying levels (e.g., medium or high) of DLIR were examined. Study end-points were assessed by 3 blinded readers and accuracy compared to invasive coronary angiography was also evaluated. Noise did not significantly differ between ASiR-V SD and DLIR-M (37 vs. 37 HU,  $p = 1.000$ ), but was significantly lower in DLIR-H (30 HU,  $p < 0.001$ ) and higher in ASiR-V HD (53 HU,  $p < 0.001$ ). Image quality was higher for DLIR-M and DLIR-H (3.4–3.8 and 4.2–4.6) compared to ASiR-V SD and HD (2.1–2.7 and 1.8–2.2;  $p < 0.001$ ), with DLIR-H yielding the highest image quality. There was no significant differences in accuracy between reconstruction methods as compared to invasive coronary angiography. This study highlights the potential of deep-learning reconstruction algorithms for improving image quality and further reducing patient radiation exposure by allowing lower acquisition doses.

Groves and colleagues performed a retrospective, cross-sectional study to assess the impact of a single energy metal artifact reduction (SEMAR) reconstruction method in 122 cardiac CT studies involving patients with implanted metal cardiac devices (pacemaker or defibrillator leads, prosthetic valves, surgical clips/markers, or spinal rods).<sup>45</sup> A defibrillator lead phantom study was also included in the analysis. Maximum beam hardening artifact radius, artifact attenuation variation surrounding the implanted metal, and image quality on a 4-point scale were assessed using standard iterative reconstruction and SEMAR. The metal artifact reduction algorithm reduced the maximum beam hardening artifact radius by 77% (standard: 14.8 mm [IQR 9.7–22.2] vs. SEMAR: 3.4 mm [IQR 2.2–7.1],  $p < 0.0001$ ) and artifact attenuation variation by 51% (standard: 130.0 HU [IQR 75.9–184.4] vs. SEMAR: 64.3 HU [IQR 48.2–89.2],  $p < 0.0001$ ). Image quality improved with SEMAR (standard: 3 [IQR 2–3.5] vs. SEMAR: 2 [IQR 1–2.5],  $p < 0.0001$ ). Similar findings were seen in the defibrillator lead phantom study.

Cardiac CTA is commonly utilized for left atrial appendage (LAA) closure planning, but current CT methods can be limited by inaccurate assessment of the LAA closure device landing zone. Bavo and colleagues assessed a computational model that was designed to simulate the deployment of 2 commonly utilized LAA closure devices in order to assess post-implantation LAA deformation and device apposition. The authors assessed 30 patients (Amulet™ = 15, Watchman™ = 15) who had undergone pre- and post-LAA closure CCT and compared software-predicted versus actual post-implant device sizes (area, perimeter, minimum and maximum diameters), apposition, and leaks on post-procedural CCT.<sup>46</sup> The authors, in this proof-of-concept study, observed very high correlation between predicted and actual post-CT device size ( $R^2 \geq 0.91$  and measurement differences all  $\leq 5\%$ ) and presence of post-device leaks.

## 7. Conclusions

The field of CCT continues to advance at a remarkable pace with expanding clinical indications and innovations. Social media, as shown by Choi et al. accelerated the dissemination of CCT knowledge from JCCT to an international audience (64% and 95% of the Twitter and Facebook audiences are outside of the United States), increased engagement, and resulted in the highest overall reach as assessed by following as compared to all other subspecialty cardiovascular imaging journals.<sup>2</sup> The diverse range of topics addressed in manuscripts, editorials, correspondences, case reports and case series, reviews, expert consensus statements and SCCT meeting abstracts published in the JCCT during 2020 are a testament to recent progress in the field and signal even more exciting years to come. The Editors are thankful to the readers, reviewers, authors, and patients who contributed to the science published in the JCCT, and who, by doing so, help to improve patient outcomes and the quality of cardiovascular medical care.

## Sources of funding

No funding was received to support this publication.

## Declaration of competing interest

Dr. Subhi Al'Aref is supported by NIH 2R01 HL12766105 and receives royalty fees from Elsevier. Dr. Armin Arbab-Zadeh received grant support from Canon. Dr. Andrew Choi holds equity in Cleerly, Inc. and receives grant support from the GW Heart and Vascular Institute. Dr. Carlo De Cecco received research support from Siemens. Dr. Damini Dey is supported by grants 1R01HL148787-01A1 and 1R01HL151266-01 and received software royalties from Cedars-Sinai Medical Center. Dr. Maros Ferencik received grant support from the National Institutes of Health and the American Heart Association. He is a consultant for Biograph, Inc. Dr. Harvey Hecht is on the scientific advisory board of Arineta and Cleerly, Inc. Dr. Jonathon Leipsic is a consultant and holds stock options in HeartFlow and Circle CVI. He is on the speakers bureau for GE Healthcare and Philips. Institutional grants from GE Healthcare, Edwards Lifesciences, Medtronic, Abbott, Boston Scientific, VMRX, and PI Cardia. Dr. Michael T. Lu MTL is supported by the American Heart Association (810966). Dr. Mohamed Marwan received speaker honoraria and is a consultant for Edwards Lifesciences. Dr. Pál Maurovich-Horvat holds stock in Neumann Medical, Ltd. Dr. Jonathan Weir-McCall is supported by the NIHR Cambridge Biomedical Research Centre (BRC-1215-20014). The views expressed are those of the author(s) and not necessarily those of the NIHR or the Department of Health and Social Care. The National Heart, Lung and Blood Institute of the National Institutes of Health has an institutional research agreement with Canon Medical Systems.

The other authors declared no relevant competing interests.

## References

- Choi AD, Parwani P, Michos ED, et al. The global social media response to the 14th annual Society of Cardiovascular Computed Tomography scientific sessions. *J Cardiovasc Comput Tomogr.* 2020;14:124–130.
- Choi AD, Feuchtnner GM, Weir-McCall J, Shaw LJ, Min JK, Villines TC. Accelerating the future of cardiac CT: social media as sine qua non? *J Cardiovasc Comput Tomogr.* 2020;14:382–385.
- Blankstein R. The impact of the COVID-19 pandemic on cardiac CT. *J Cardiovasc Comput Tomogr.* 2020;14:209–210.
- Mahmud E, Dauerman HL, Fgg Welt, et al. Management of acute myocardial infarction during the COVID-19 pandemic: a position statement from the society for cardiovascular angiography and interventions (SCAI), the American College of Cardiology (ACC), and the American College of emergency physicians (ACEP). *J Am Coll Cardiol.* 2020;76:1375–1384.
- The European Society for Cardiology. ESC guidance for the diagnosis and management of CV disease during the COVID-19 pandemic (Last update: 10 June 2020) <https://www.escardio.org/Education/COVID-19-and-Cardiology/ESCCOVID-19-Guidance>.
- Choi AD, Abbara S, Branch KR, et al. Society of cardiovascular computed tomography guidance for use of cardiac computed tomography amidst the COVID-19 pandemic endorsed by the American College of Cardiology. *J Cardiovasc Comput Tomogr.* 2020;14:101–104.
- Farooqi KM, Ghoshhajra BB, Shah AM, et al. Recommendations for risk stratified use of cardiac computed tomography for congenital heart disease during the COVID-19 pandemic. *J Cardiovasc Comput Tomogr.* 2020;14:291–293.
- Hecht HS, Blaha MJ, Kazerooni EA, et al. CAC-DRS: coronary artery calcium data and reporting system. An expert consensus document of the society of cardiovascular computed tomography (SCCT). *J Cardiovasc Comput Tomogr.* 2018;12:185–191.
- Dzaye O, Dudum R, Mirbolouk M, et al. Validation of the coronary artery calcium data and reporting system (CAC-DRS): dual importance of CAC score and CAC distribution from the coronary artery calcium (CAC) consortium. *J Cardiovasc Comput Tomogr.* 2020;14:12–17.
- Cury RC, Abbara S, Achenbach S, et al. CAD-RADS(TM) coronary artery disease - reporting and data system. An expert consensus document of the society of cardiovascular computed tomography (SCCT), the American College of radiology (ACR) and the north American society for cardiovascular imaging (NASCI). Endorsed by the American College of Cardiology. *J Cardiovasc Comput Tomogr.* 2016;10:269–281.
- Williams MC, Moss A, Dweck M, et al. Standardized reporting systems for computed tomography coronary angiography and calcium scoring: a real-world validation of CAD-RADS and CAC-DRS in patients with stable chest pain. *J Cardiovasc Comput Tomogr.* 2020;14:3–11.
- de Ronde MWJ, Khoshiwal A, Planken RN, et al. A pooled-analysis of age and sex based coronary artery calcium scores percentiles. *J Cardiovasc Comput Tomogr.* 2020;14:414–420.
- Senoner T, Plank F, Beyer C, et al. Does coronary calcium score zero reliably rule out coronary artery disease in low-to-intermediate risk patients? A coronary CTA study. *J Cardiovasc Comput Tomogr.* 2020;14:155–161.



14. Goehler A, Mayrhofer T, Pursnani A, et al. Long-term health outcomes and cost-effectiveness of coronary CT angiography in patients with suspicion for acute coronary syndrome. *J Cardiovasc Comput Tomogr.* 2020;14:44–54.
15. van den Hoogen IJ, van Rosendael AR, Lin FY, et al. Coronary atherosclerosis scoring with semiquantitative CCTA risk scores for prediction of major adverse cardiac events: propensity score-based analysis of diabetic and non-diabetic patients. *J Cardiovasc Comput Tomogr.* 2020;14:251–257.
16. Ahmadi A, Senoner T, Correa A, Feuchtnr G, Narula J. How atherosclerosis defines ischemia: atherosclerosis quantification and characterization as a method for determining ischemia. *J Cardiovasc Comput Tomogr.* 2020;14:394–399.
17. Kolossvary M, De Cecco CN, Feuchtnr G, Maurovich-Horvat P. Advanced atherosclerosis imaging by CT: radiomics, machine learning and deep learning. *J Cardiovasc Comput Tomogr.* 2019;13:274–280.
18. Lin FY, Villines TC, Narula J, Shaw LJ. What is the clinical role of non-invasive atherosclerosis imaging? *J Cardiovasc Comput Tomogr.* 2019;13:261–266.
19. Nakanishi R, Motoyama S, Leipsic J, Budoff MJ. How accurate is atherosclerosis imaging by coronary computed tomography angiography? *J Cardiovasc Comput Tomogr.* 2019;13:254–260.
20. van Rosendael AR, Lin FY, Ma X, et al. Percent atheroma volume: optimal variable to report whole-heart atherosclerotic plaque burden with coronary CTA, the PARADIGM study. *J Cardiovasc Comput Tomogr.* 2020;14:400–406.
21. Foldyna B, Lo J, Mayrhofer T, Grinspoon SK, Hoffmann U, Lu MT. Individual coronary plaque changes on serial CT angiography: within-patient heterogeneity, natural history, and statin effects in HIV. *J Cardiovasc Comput Tomogr.* 2020;14:144–148.
22. Mushtaq S, Conte E, Pontone G, et al. Interpretability of coronary CT angiography performed with a novel whole-heart coverage high-definition CT scanner in 300 consecutive patients with coronary artery bypass grafts. *J Cardiovasc Comput Tomogr.* 2020;14:137–143.
23. Ahn JH, Jeong YH, Park Y, et al. Head-to-head comparison of prognostic accuracy in patients undergoing noncardiac surgery of dobutamine stress echocardiography versus computed tomography coronary angiography (PANDA trial): a prospective observational study. *J Cardiovasc Comput Tomogr.* 2020;14:471–477.
24. Hull RA, Berger JM, Boster JM, et al. Adoption of coronary artery disease - reporting and Data System (CAD-RADS) and observed impact on medical therapy and systolic blood pressure control. *J Cardiovasc Comput Tomogr.* 2020;14:421–427.
25. Almeida S, Pelter M, Shaikh K, et al. Feasibility of measuring pericoronary fat from precontrast scans: effect of iodinated contrast on pericoronary fat attenuation. *J Cardiovasc Comput Tomogr.* 2020;14:490–494.
26. Patel AR, Bamberg F, Branch K, et al. Society of cardiovascular computed tomography expert consensus document on myocardial computed tomography perfusion imaging. *J Cardiovasc Comput Tomogr.* 2020;14:87–100.
27. Singh A, Mor-Avi V, Patel AR. The role of computed tomography myocardial perfusion imaging in clinical practice. *J Cardiovasc Comput Tomogr.* 2020;14:185–194.
28. Nieman K, Balla S. Dynamic CT myocardial perfusion imaging. *J Cardiovasc Comput Tomogr.* 2020;14:303–306.
29. Mushtaq S, Conte E, Pontone G, et al. State-of-the-art-myocardial perfusion stress testing: static CT perfusion. *J Cardiovasc Comput Tomogr.* 2020;14:294–302.
30. Yi Y, Xu C, Wu W, et al. Stress dynamic myocardial CT perfusion for symptomatic patients with intermediate- or high-risk of coronary artery disease: optimization and incremental improvement between the absolute and relative myocardial blood flow analysis. *J Cardiovasc Comput Tomogr.* 2020;14:437–443.
31. Yi Y, Xu C, Wu W, et al. Myocardial blood flow analysis of stress dynamic myocardial CT perfusion for hemodynamically significant coronary artery disease diagnosis: the clinical value of relative parameter optimization. *J Cardiovasc Comput Tomogr.* 2020;14:314–321.
32. Samady H, Molony DS, Coskun AU, Varshney AS, De Bruyne B, Stone PH. Risk stratification of coronary plaques using physiologic characteristics by CCTA: focus on shear stress. *J Cardiovasc Comput Tomogr.* 2020;14:386–393.
33. Mizukami T, Tanaka K, Sonck J, et al. Evaluation of epicardial coronary resistance using computed tomography angiography: a Proof Concept. *J Cardiovasc Comput Tomogr.* 2020;14:177–184.
34. Jochheim D, Deseive S, Schwendtner S, et al. Impact of severe left ventricular outflow tract calcification on device failure and short-term mortality in patients undergoing TAVI. *J Cardiovasc Comput Tomogr.* 2020;14:36–41.
35. Pollari F, Hitzl W, Vogt F, et al. Aortic valve calcification as a risk factor for major complications and reduced survival after transcatheter replacement. *J Cardiovasc Comput Tomogr.* 2020;14:307–313.
36. Weir-McCall JR, Attinger-Toller A, Blanke P, et al. Annular versus supra-annular sizing for transcatheter aortic valve replacement in bicuspid aortic valve disease. *J Cardiovasc Comput Tomogr.* 2020;14:407–413.
37. Fukui M, Xu J, Abdelkarim I, et al. Global longitudinal strain assessment by computed tomography in severe aortic stenosis patients - feasibility using feature tracking analysis. *J Cardiovasc Comput Tomogr.* 2019;13:157–162.
38. Gegenava T, van der Bijl P, Hirasawa K, et al. Feature tracking computed tomography-derived left ventricular global longitudinal strain in patients with aortic stenosis: a comparative analysis with echocardiographic measurements. *J Cardiovasc Comput Tomogr.* 2020;14:240–245.
39. Fukui M, Xu J, Thoma F, et al. Baseline global longitudinal strain by computed tomography is associated with post transcatheter aortic valve replacement outcomes. *J Cardiovasc Comput Tomogr.* 2020;14:233–239.
40. Cavallo AU, Patterson AJ, Thomas R, et al. Low dose contrast CT for transcatheter aortic valve replacement assessment: results from the prospective SPECTACULAR study (spectral CT assessment prior to TAVR). *J Cardiovasc Comput Tomogr.* 2020;14:68–74.
41. Massalha S, Almuefleh A, Walpot J, et al. Reference values for mid-diastolic right ventricular volume in population referred for cardiac computed tomography: an additional diagnostic value to cardiac computed tomography. *J Cardiovasc Comput Tomogr.* 2020;14:226–232.
42. Morris MF, Pena Jr A, Kalya A, et al. Predicting paravalvular leak after transcatheter mitral valve replacement using commercially available software modeling. *J Cardiovasc Comput Tomogr.* 2020;14:495–499.
43. Vingiani V, Abadia AF, Schoepf UJ, et al. Low-kV coronary artery calcium scoring with tin filtration using a kV-independent reconstruction algorithm. *J Cardiovasc Comput Tomogr.* 2020;14:246–250.
44. Benz DC, Benetos G, Rampidis G, et al. Validation of deep-learning image reconstruction for coronary computed tomography angiography: impact on noise, image quality and diagnostic accuracy. *J Cardiovasc Comput Tomogr.* 2020;14:444–451.
45. Groves DW, Acharya T, Steveson C, et al. Performance of single-energy metal artifact reduction in cardiac computed tomography: a clinical and phantom study. *J Cardiovasc Comput Tomogr.* 2020;14:510–515.
46. Bavo AM, Wilkins BT, Garot P, et al. Validation of a computational model aiming to optimize preprocedural planning in percutaneous left atrial appendage closure. *J Cardiovasc Comput Tomogr.* 2020;14:149–154.

Todd C. Villines\*

University of Virginia Health System, Charlottesville, VA, USA

Subhi J. Al'Aref

University of Arkansas for Medical Sciences, Little Rock, AR, USA

Daniele Andreini

Centro Cardiologico Monzino, IRCCS, Milan, Italy

Marcus Y. Chen

National Heart, Lung and Blood Institute, Bethesda, MD, USA

Andrew D. Choi

The George Washington University School of Medicine, Washington, DC, USA

Carlo N. De Cecco

Emory University, Atlanta, GA, USA

Damini Dey

Cedars Sinai Medical Center, Los Angeles, CA, USA

James P. Earls

The George Washington University School of Medicine, Washington, DC, USA

Maros Ferencik

Oregon Health and Science University, Portland, OR, USA

Heidi Gransar

Cedars Sinai Medical Center, Los Angeles, CA, USA

Harvey Hecht

Icahn School of Medicine at Mount Sinai, New York, NY, USA

Jonathon A. Leipsic

University of British Columbia, Vancouver, BC, Canada

Michael T. Lu

Cardiovascular Imaging Research Center, Massachusetts General Hospital and Harvard Medical School, USA

Mohamed Marwan

Friedrich-Alexander University Erlangen-Nürnberg, Germany

Pál Maurovich-Horvat

Medical Imaging Center, Semmelweis University, Budapest, Hungary

Edward Nicol

Royal Brompton Hospital, London, UK

Gianluca Pontone

Centro Cardiologico Monzino, IRCCS, Milan, Italy

Jonathan Weir-McCall

University of Cambridge, Cambridge, UK

Seamus P. Whelton

Johns Hopkins University School of Medicine, Baltimore, MD, USA

Michelle C. Williams

*The University of Edinburgh, Edinburgh, UK*

Armin Arbab-Zadeh

*Johns Hopkins University School of Medicine, Baltimore, MD, USA*

Gudrun M. Feuchtner

*Innsbruck Medical University, Innsbruck, Austria*

\* Corresponding author. Julian Beckwith Ruffin Professor of Medicine,  
Division of Cardiovascular Medicine, 1215 Lee Street, University of  
Virginia Health System, Charlottesville, VA, 22908, USA.  
E-mail address: [tv4bc@virginia.edu](mailto:tv4bc@virginia.edu) (T.C. Villines).